Dielectric properties and photoluminescence of calcium stannate titanate doped with europium

XINQIAO TENG[1], YUN ZHOU[1,*], SIYU YANG[1], SUSU WANG[1], HAOMIAO ZHOU[2]
[1]*College of Science, China Jiliang University, Hangzhou 310018, China*
[2]*College of Information Engineering, China Jiliang University, Hangzhou 310018, China*

Tin-containing calcium titanate materials have attracted much attention since they can reduce the exciton binding energy and increase the carrier mobility of their related compounds. Eu-doped $CaTi_{0.995}Sn_{0.005}O_3$ ceramics were synthesized by a solid-state reaction. The structure and dielectric properties of the materials were characterized by X-ray diffractometer, SEM, and LCR meter; while the optical properties of the materials were characterized by Raman, UV-VIS, and fluorescence spectroscopy. The results show that the dielectric constant, dielectric loss, absorbance, and luminescence intensity increase with the increase of the rare earth metal doping concentration.

(Received November 1, 2021; accepted June 6, 2022)

Keywords: Rare earth doping, Solid-state reaction, Dielectric property, Photoluminescence

1. Introduction

In recent years, rare earth metals have been widely used for doping into various substances for modification. In this context, a previous study by Dong and Da [1] showed that the rare earth doped (Ho^{3+}) dielectric material $BaTiO_3$ can not only effectively improve its dielectric properties, but also enhance its luminescence properties. Due to the abundant titanium resources, low price of raw materials, and stable physical and chemical properties, the research on dielectric materials based on the titanate matrix is relatively extensive [2]. In addition, the anionic group of this type of material has a sensitizing effect, which can efficiently absorb excitation energy and transfer it to the rare earth ions to make it emit light. Compounds that exhibit this type of behavior represent a new type of functional material and have drawn much research interest, due to their attractive physical properties, high luminous efficiency, and wide applications in many multifunctional devices [3]. Calcium titanate ($CaTiO_3$) is one of the most typical ABO_3 perovskite oxides [4]. Its structure can be distorted due to external pressure or chemical substitution. This lattice distortion greatly reduces the symmetry of the crystal, which in turn reduces the symmetry of the lattice environment of the rare earth cation (RE^{3+}) doped into the crystal lattice, enhancing the 4*f*-4*f* transition of RE^{3+} ions [4]. It has been widely used as a host for phosphors for good chemical stability [5-6]. Other documents indicate that tin-based perovskite materials have more superior optoelectronic semiconductor properties, such as narrower band gap width, low exciton binding energy, higher carrier mobility, which have garnered them much attention [7]. In addition, research has shown that doping a small amount of Sn in calcium titanate is beneficial to improve the luminescence properties of the material. For example, Tang et al reported that the maximum luminosity was attained in Sn-doped $CaTiO_3$ when the doping concentration was 0.005% (molar ratio) [8]. This is mainly because the addition of Sn will make the migration state of the intermediate charge and its conduction band have an energy position that allows the 4*f*5*d* band to efficiently capture electrons [8]. Currently, extensive research has been done on the red phosphor calcium titanate matrix doped with rare-earth ions, but it is mainly focused on Pr^{3+} doping and on the phosphor long afterglow [9]. The rare-earth ion Eu^{3+} has excellent red luminescence characteristics. It is considered as one of the best candidates for its use in photonic applications as red-emitting phosphors among lanthanide ions [10]. However, the practical application of its luminous intensity distance is still underexplored [11]. Based on the above considerations, we choose to study the calcium titanate material with a tin concentration of 0.005% (molar ratio) as our research focus and use Eu^{3+} for trace doping to investigate the structure, dielectric, and optical properties of the material.

2. Experimental details

Eu-doped $CaTi_{0.995}Sn_{0.005}O_3$ ceramics were synthesized by the solid-phase reaction method. The mol percentage of Eu to the total amount of Eu and Ca (x) was varied from 0 to 3% (x=0, 1, 2, 3 mol%). First, the raw materials SnO_2 (99.5%), TiO_2 (99.8%), $CaCO_3$ (99.99%), and Eu_2O_3 (99.99%) were weighted and dried in a blast drying oven at 105 °C for 4 h to remove the adsorbed water. The reagents were mixed with an appropriate amount of ethanol and put into a ball mill tank. The powder, the grinding balls, and the ethanol occupied a

space about two-thirds of the ball mill tank. The ball mill operated at a frequency of 320 r/min for 12 hours. After the ball milling program was completed, the grinding balls were removed and the resulting ground powder was placed in a blast drying oven to remove the residual ethanol for 24 hours. After the drying was completed, the powder was placed into a crucible for pre-sintering at 850 °C for 3 h. After the pre-sintering, the sample was cooled down and transferred to a mortar. Polyvinyl alcohol (PVA) was added to the mortar at a ratio of 3:2 and the mixture was ground thoroughly. After this process was finished, the powder was pressed into 5 mm diameter and 1 mm thick pellets using a hydraulic press with the pressure of 8 MPa, followed by placing the pellets in a high-temperature oven. The adhesion was discharged in an environment of 550 °C for 10 h to remove the moisture from the PVA addition. After the debonding, the sample was sintered under air at a temperature of 1150 °C for 3 h. Finally, Eu-doped $CaTi_{0.995}Sn_{0.005}O_3$ ceramics with different concentrations (x=0, 1, 2, 3 mol%) was obtained.

The samples were analyzed by an X-ray diffractometer (Bruker D8 XRD) to verify the crystallinity of the samples; an RT1-PremierII ferroelectric tester to detect the ferroelectricity of the samples; an LCR comprehensive tester model ZM2353 to detect the dielectric properties; a Raman spectrometer (Renishaw inVia) of British Renishaw to access the Raman spectra; a Shimadzu UV-3600 UV-visible spectrophotometer to measure the UV absorption of the samples; a Fluorolog-3 fluorescence spectrometer to detect the luminescence properties of doped materials.

3. Results and discussion

X-ray diffraction was used to determine the structural characteristics of the sample. Fig. 1 shows the XRD patterns of different concentrations of Eu_2O_3 doped samples that were calcined at 1150 °C. It can be seen from this figure that all the diffraction peaks correspond to the structure of the orthogonal $CaTiO_3$, and no stray peaks corresponding to other structures are observed. This shows that the trace doping of rare-earth ions does not affect the main structure of $CaTiO_3$. Additionally, it also shows that all Eu^{3+} enters the $CaTi_{0.995}Sn_{0.005}O_3$ lattice. Table 1 lists the lattice parameters of the doped samples, and shows that the *a*-axis values of the doped samples are significantly reduced, while the *c*-axis values increased, and the unit cell volume is significantly higher.

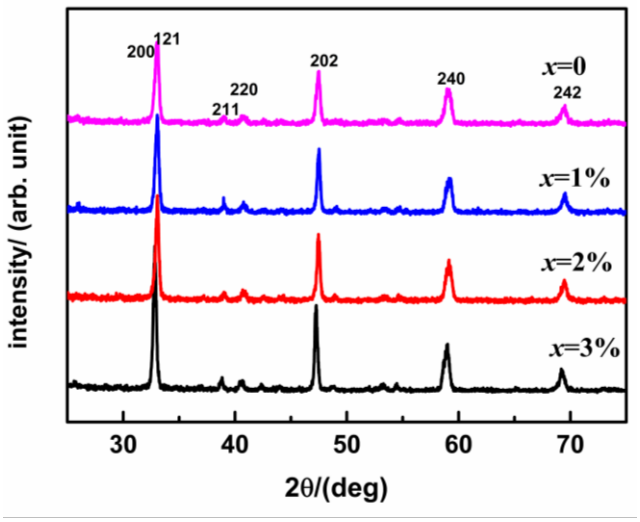

Fig. 1. X-ray diffraction patterns of $CaTi_{0.995}Sn_{0.005}O_3$ ceramics doped at different Eu^{3+} concentrations (color online)

Table 1. Data on lattice parameters of $CaTi_{0.995}Sn_{0.005}O_3$ ceramics doped at different Eu^{3+} concentrations

x	a (Å)	b (Å)	c (Å)	Cell volume ($Å^3$)	X-ray density (g/cm^3)
0	5.4663	7.6305	5.2656	219.63	4.1123
0.1	5.4273	7.6462	5.3983	224.02	4.0317
0.2	5.4271	7.6360	5.3874	223.26	4.0454
0.3	5.4329	7.6511	5.3965	224.32	4.0263

The dielectric and photoluminescence properties of the samples depend on their microstructure. Thus, it is necessary to study the microstructure characteristics of the samples. Fig. 2 shows the series SEM micrographs of the Eu-doped $CaTi_{0.995}Sn_{0.005}O_3$ ceramics with the concentrations (a) x =0 and (b) x = 0.1. The ceramic shows a homogeneous microstructure. The average grain size observed in these ceramics is about 0.3 μm.

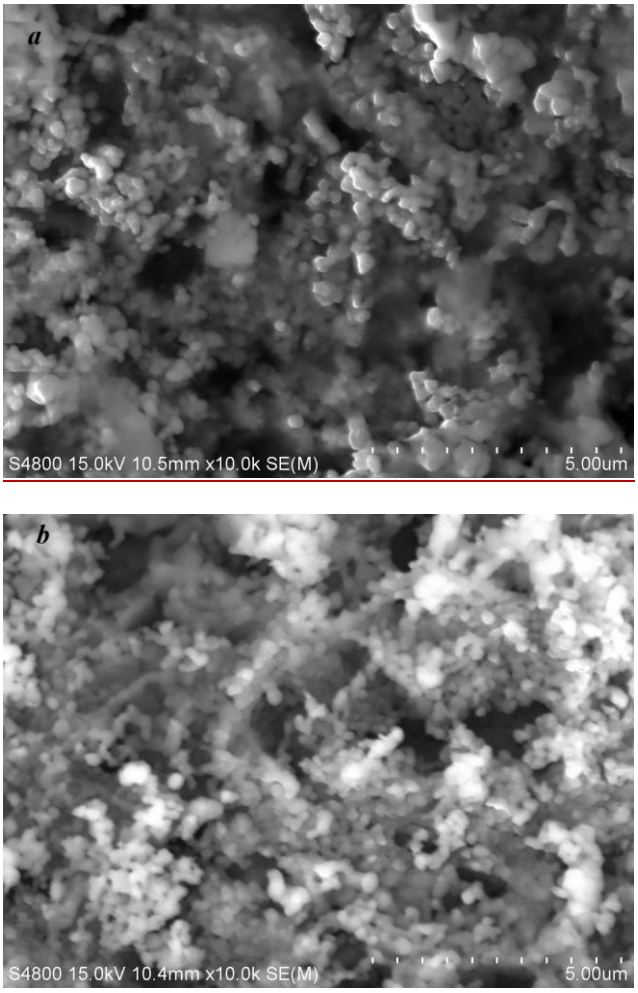

Fig. 2. SEM micrographs of $CaTi_{0.995}Sn_{0.005}O_3$ ceramics doped Eu^{3+} concentrations with (a) x = 0 and (b) x = 0.1

Fig. 3 shows the relative permittivity (ε_r) of different doped samples as a function of frequency. It can be observed different doped samples show similar trends when the frequency increases. That is, at low frequencies, the relative permittivity decreases significantly. As the frequency increases further, the value of the relative permittivity decreases gradually and becomes constant. It is also observed that the relative permittivity of the doped samples is significantly higher than that of the non-doped sample. As the doping concentration increases, the dielectric constant values of the samples also increase.

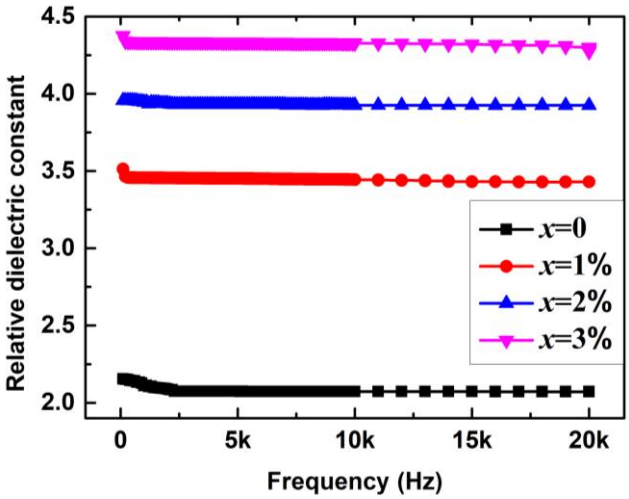

Fig. 3. Frequency-dependent variation of relative dielectric constant for $CaTi_{0.995}Sn_{0.005}O_3$ ceramics doped at different Eu^{3+} concentrations at room temperature (color online)

Fig. 4 shows the relationship between the dielectric loss of the doped samples and the frequency. It is observed that all the four samples showed the same trend: as the frequency increases, the value of the loss tangent decreases sharply, and as the frequency further increases, the value of the loss tangent reaches a plateau, followed by a gentle decrease. Simultaneously, the dielectric loss tends to rise with the increase of the doping concentration. This result indicates that at higher doping levels, Eu is apt to cause electrical conductivity of $CaTi_{0.995}Sn_{0.005}O_3$ [12]. Additionally, the dielectric loss values of these four samples are relatively small, indicating that the dielectric properties of the samples are good.

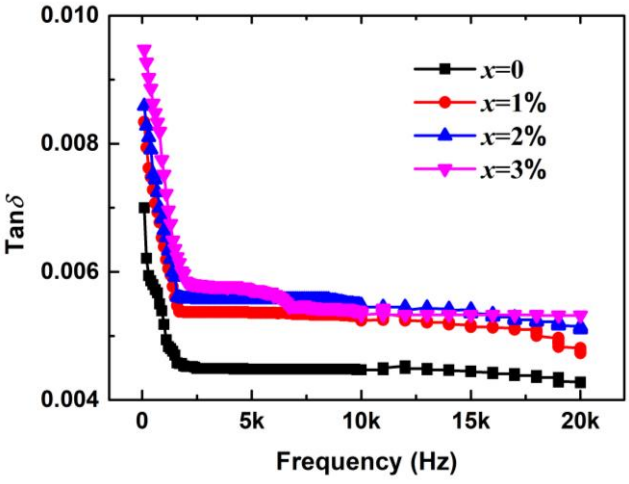

Fig. 4. Frequency-dependent variation of dielectric loss for $CaTi_{0.995}Sn_{0.005}O_3$ ceramics doped at different Eu^{3+} concentrations at room temperature (color online)

Fig. 5 shows the Raman spectra of the four samples with a laser emission wavelength of 532 nm. It can be seen from the figure that the Raman spectra of $CaTi_{0.995}Sn_{0.005}O_3$ with doping is very different from that of $CaTi_{0.995}Sn_{0.005}O_3$ without doping. This shows that these peaks are caused by the doping of rare-earth europium. Furthermore, it can be seen that as the doping concentration increases, the peak intensity also increases. This phenomenon shows that even a small amount of rare earth doping can be detected, showing that Raman spectroscopy is an effective and sensitive method for detecting rare earth traces in doped samples.

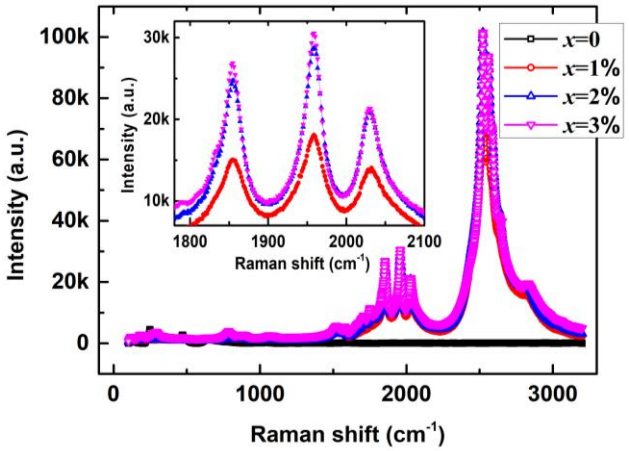

Fig. 5. Raman spectra of $CaTi_{0.995}Sn_{0.005}O_3$ ceramics doped at different Eu^{3+} concentrations at room temperature (color online)

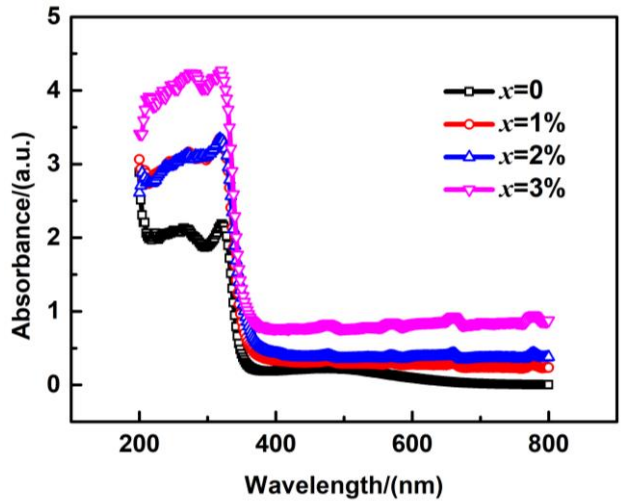

Fig. 6. Emission spectrum of $CaTi_{0.995}Sn_{0.005}O_3$ ceramics doped at different Eu^{3+} concentrations at room temperature (color online)

UV-visible light spectrometry was used to measure the non-doped and doped samples. As observed in Fig. 6, all four samples show strong absorption properties in the ultraviolet range from 200–330 nm. As the wavelength of the light increases, the absorbance decreases steadily. As the doping concentration of europium increases, the absorbance of the sample gradually increases. The main absorption peak is located near the wavelength of 320 nm. In addition, the three doped samples have obvious absorption peaks at 478 nm, 570 nm, 660 nm, and 778 nm. This may be caused by the transition of the coordination field of the lanthanide element. That is, after absorbing a certain energy photon, the *f* electron in the *f* orbital of the Eu element transitions from the *f* orbital low-energy state to the *f*-orbital high-energy state, generating the absorption spectrum. It is worth pointing out that the strong absorption performance of rare earth element doped samples in the ultraviolet region indicates that such materials may be used to produce sunscreen products.

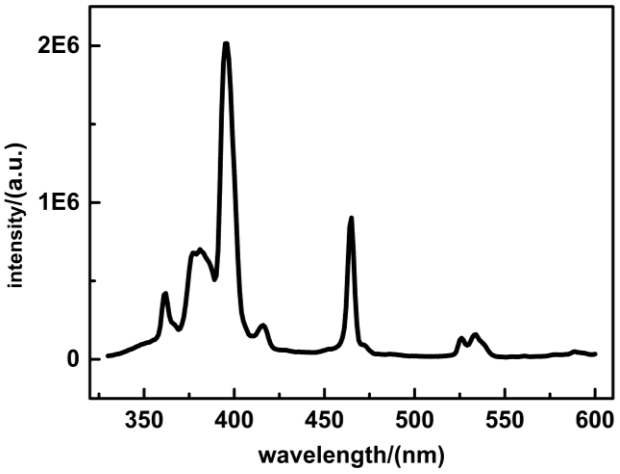

Fig. 7. Excitation spectrum of $CaTi_{0.995}Sn_{0.005}O_3$ ceramics doped Eu^{3+} concentration with *x*=1% *at room temperature*

In order to clarify the reaction of the material to the external light excitation, we tested the excitation spectrum of the sample doped at 1%, as shown in Fig. 7. It can be seen that the excitation spectrum is mainly composed of two strong peaks. The main excitation peaks are respectively 397 nm and 465 nm. They represent the spectral line composition of the *ff* transition of Eu^{3+}, corresponding to the electronic transition from the ground state level $^7F_0$ of Eu^{3+} to the excited state $^5D_2$ and $^5L_6$ energy levels. That is, they are due to the $^7F_0 \rightarrow {}^5L_6$, and to the $^7F_0 \rightarrow {}^5D_2$ transitions of Eu^{3+} [13]. Furthermore, the doping of Eu^{3+} into the $CaTiO_3$ material partially replaces the Ca^{2+} in the matrix. However, the mismatch of charge and valence may affect the luminescence performance of the synthetic material, as reported in some references [14-15].

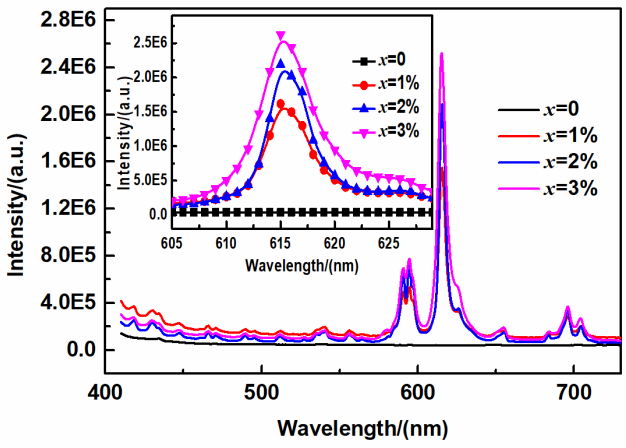

Fig. 8. Emission spectrum of $CaTi_{0.995}Sn_{0.005}O_3$ ceramics doped at different Eu^{3+} concentrations at room temperature (color online)

We further detected the emission spectra of Eu-doped $CaTi_{0.995}Sn_{0.005}O_3$ ceramics, as shown in Fig. 8. In this experiment, we excited the sample with an excitation wavelength of 395 nm. It can be seen that the non-doped sample has no obvious emission peaks, while the emission spectra of the doped samples are very similar. The latter show emission peaks at 589 nm, 615 nm, and 652 nm of Eu^{3+}, corresponding to the transitions: $^5D_0 \rightarrow {}^7F_1$, $^5D_0 \rightarrow {}^7F_2$, and $^5D_0 \rightarrow {}^7F_3$, respectively. Importantly, the main peak transition emission at 615 nm corresponds to the $^5D_0 \rightarrow {}^7F_2$ energy level. This indicates that the electric dipole moment transition is the main mode of spectral emission [16]. In addition, we also found that as the doping concentration increases, the intensity of the emission spectrum increases. The inset in Fig. 8 reflects the emission peak of the sample at 615 nm. Evidently, as the doping concentration increases, the related peak also increases, showing that the luminescence intensity of low concentration doped samples increases with the increase of the doping concentration.

4. Conclusions

In this paper, a solid-phase reaction method was used to prepare rare earth europium-doped tin-containing calcium titanate, and the structure, dielectric properties, and optical properties of the ceramic samples were tested. The experimental results show that low-concentration europium doping can significantly improve the light absorption and luminescence properties of the material. Furthermore, the dielectric constant, the dielectric loss, the absorbance, and the luminescence intensity increase with the increase of the doping concentration.

Acknowledgment

The work is supported by Zhejiang Provincial Natural Science Foundation of China (Nos. LY21F010010, LZ19A020001), National Natural Science Foundation of China (No. 11972333).

References

[1] Y. L. Da, X. G. Dong, Sci. Rep. **7**(1), 6125 (2017).
[2] K. J. Choi, Science **306**(5698), 1005 (2004).
[3] P. Liu, J. Yin, X. Mi, L. Zhang, L. Bie, Journal of Rare Earths **31**(6), 555 (2013).
[4] D. Sando, Journal of Physics: Condensed Matter. **34**, 153001 (2022).
[5] S. Vasconcelos, M. Silva, R. Oliveira, M. Bezerra Junior, H. Andrade, I. Queiroz Junior, C. Singh, A. Sombra, Materials Chemistry and Physics **257**, 123239 (2020).
[6] V. V. Shanbhag, S. C. Prashantha, C. R. Ravikumar, P. Kumar, B. S. Surendra, H. Nagabhushana, D. M. Jnaneshwara, V. Revathi, Ramachandra Naik, T. S. Shashidhara, Y. G. Krupanidhi, Inorganic Chemistry Communications **134**, 108960 (2021).
[7] L. M. Herz, Journal of Physical Chemistry Letters **9**(23), 6853 (2018).
[8] M. Tang, X. Wang X. Y. Xi, Sciencepaper Online **6**(02), 157 (2011).
[9] H. J. Guo, Y. H. Wang, G. Li, J. Liu, P. Feng, D. W. Liu, J. Mater. Chem. C **5**(11), 2844 (2017).
[10] R. E. Bahi, M. Dammak, W. Donner, A. Njeh, Journal of Luminescence **237**, 118176 (2021).
[11] W. Hai Feng, L. Jian Wei, W. Ruo Xuan, D. Yun Gu, D. Lin Feng, Materials **13**(4), 874 (2020).
[12] D.-Y. Lu, X.-Y. Sun, B. Liu, J.-L. Zhang, T. Ogata, Journal of Alloys and Compounds **615**, 25 (2014).
[13] C. Sheng-Hong, T. Wei, C. Rui, W. Qingmeng, Y. Jian Hui, F. Qiang, Neijiang Science and Technology **39**(11), 102 (2018).
[14] P. Wang, J. Mao, X. Wei, L. Qiu, B. Jiang, F. Chi, M. Yin, Y. Chen, Journal of Alloys and Compounds **869**, 159277 (2021).
[15] X. Wang, X. Wang, Q. Di, H. Zhao, B. Liang, J. Yang, Materials **10**(12), 1398 (2017).
[16] F. Chun-Yang, Z. Wen-Xun, B. Kai-Yang, S. Zhen, Z. Lu Yao, L. Qin, Chem. Eng. J. **255**(12), 9 (2016).

*Corresponding author: zhouyun@cjlu.edu.cn